

Determining topological order from a local ground-state correlation function

Zohar Ringel and Yaacov E. Kraus

Department of Condensed Matter Physics, Weizmann Institute of Science, Rehovot 76100, Israel

Topological insulators are physically distinguishable from normal insulators only near edges and defects, while in the bulk there is no clear signature to their topological order. In this work we show that the \mathbb{Z}_2 index of topological insulators and the \mathbb{Z} index of the integer quantum Hall effect manifest themselves locally. We do so by providing an algorithm for determining these indices from a local equal time ground-state correlation function at any convenient boundary conditions. Our procedure is unaffected by the presence of disorder and can be naturally generalized to include weak interactions. The locality of these topological indices implies bulk-edge correspondence theorem.

PACS numbers: 73.43.-f, 73.43.Cd, 73.20.-r, 71.23.-k

I. INTRODUCTION

The theoretical proposal and experimental discovery of topological band insulators [1] (TI) has been raising increasing interest in the condensed matter physics community. These materials form a novel topological state of matter, which does not fall into the standard classification of broken symmetries. Instead, what distinguishes this phase from a trivial band insulator (BI) is the existence of a nontrivial \mathbb{Z}_2 topological index associated with the full band structure. This distinction is somewhat analogous to the integer quantum Hall effect (IQHE), whose distinguished states can be attributed to a \mathbb{Z} topological index associated with full Landau levels of noninteracting electrons.

Broken symmetry phases are characterized by local order parameters, in what is known as the Landau paradigm [2]. It is commonly accepted that this paradigm does not apply to the above topological phases. Instead, such phases are described by the more elusive quantity, known as a topological order [3].

In IQHE the quantized Hall conductance is a direct manifestation of the topological order, and for the case of free electrons, this response function is a local bulk quantity [4]. As far as we know, for TI the implication of the topological order is only through edge effects (see, for example, Refs. [5–7]) or defect-related effects [8]. There is no local response function that is known to characterizes this \mathbb{Z}_2 phase, let alone an order parameter.

In this work we show that both the \mathbb{Z}_2 index of the TI and the \mathbb{Z} index of the IQHE, as well as any gapped insulator with non-zero Chern number ν , can be extracted from a local equal time ground-state correlation function. This implies that *in these systems the topological order is in fact a local ground state property*. It also proves a bulk-edge correspondence theorem for such local topological orders.

When interactions are taken into account, the \mathbb{Z} index remains well defined [9], while it is yet unclear whether the \mathbb{Z}_2 index does [10, 11]. Our formulation, however, remains well defined at least for weak interactions, and thus suggests an extension to the definition of the TI to weakly interacting systems. Beyond weak interactions,

we show that either the energy gap or some “occupation gap” must be closed during the transition from a TI to a BI.

The theoretical procedure that we provide can be straightforwardly adapted to form an algorithm for numerically determining the \mathbb{Z}_2 and \mathbb{Z} indices. This algorithm is rather efficient, since one only needs to diagonalize several matrices with dimensions of the order of the correlation length squared (2D) or cubed (3D). Such an algorithm may help in numerically testing a predicted topological order.

II. FINDING LOCALLY THE TOPOLOGICAL ORDER

Our procedure of extracting the topological index deals with noninteracting lattice-based band insulators. The required input is the equal time ground-state two-point correlation function

$$P_{ij} = \langle gs | \psi_i^\dagger \psi_j | gs \rangle, \quad (1)$$

where $|gs\rangle$ is the many body ground state, and ψ_i^\dagger (ψ_i) is the creation (annihilation) operator of an electron in site i (for brevity we let i encompass also the orbital and spin degrees of freedom). For noninteracting electrons the two-point correlation function coincides with the single-particle spectral projector

$$P_{ij} = \sum_{E_n < \mu} \langle i | n \rangle \langle n | j \rangle, \quad (2)$$

where $|i\rangle$ is the single-particle wave function associated with ψ_i^\dagger , $|n\rangle$ is an eigenstate of the single-particle Hamiltonian with an energy E_n , and μ is the chemical potential. Since we are interested in local bulk properties, we assume that the sites i and j reside within the bulk.

In the following (see Property I below) we show that P_{ij} is exponentially local, namely it decays exponentially with the distance between i and j within some correlation length l_p and has only an exponentially small dependence on details of the Hamiltonian outside a local region around i and j . This locality allows us to discuss P_{ij}

within some given \mathcal{A} , without concerning ourselves with details of the edges of the region, boundary conditions, or the Hamiltonian outside \mathcal{A} . In particular, for any geometry of \mathcal{A} , we can always consider a subregion with a geometry of a Corbino disk, or a thick torus (Corbino donut) in 3D, which we assume to have circumferences larger than l_p .

Given P on such a region, we multiply P_{ij} by a geometric phase factor, in a way that we call “artificial flux insertion”

$$P_{ij}(\phi) = P_{ij}e^{i\theta_{ij}\phi}, \quad (3)$$

where $\phi \in \mathbb{R}$ and $\theta_{ij} \in (-\pi, \pi]$ is the azimuthal angle from site i to site j . In the proceeding we assume for convenience that in 2D \mathcal{A} is of the topologically equivalent cylindrical geometry.

A key analytical result in this work (Property II) is that Eq. (3) captures the effect of real magnetic flux insertion, up to $O(e^{-L/l_p})$ corrections, where L is the inner circumference of the Corbino disk (or donut). Hence the inclusion of flux is merely a transformation of P , which yields no extra information in addition to the information already contained in P [12].

The next step is to construct 1D Wannier functions out of P . Let X be the position operator along the open coordinate \hat{x} . We define the 1D Wannier functions $|w_n(\phi)\rangle$ to be the eigenstates of the projected position operator in a given flux [13]

$$PXP|_{\phi}|w_n(\phi)\rangle = x_n(\phi)|w_n(\phi)\rangle. \quad (4)$$

This definition of the Wannier functions has several advantages. First, it relies on P rather than the Bloch wave functions, hence the eigenvalues x_n are unaffected by the phase freedom in Fourier space, on the one hand, and it remains defined in the presence of disorder, on the other hand. Second, since $P(\phi)$ is a continuous function of ϕ , the x_n 's are also continuous in ϕ . Third, in time-reversal-preserving systems $PXP|_{\phi}$ is a time-reversal-invariant operator for $\phi = 0, \pi$, and thus Kramers' theorem assures that the Wannier functions come in time-reversal pairs with doubly degenerate eigenvalues at these points. Last, we prove below (Property III) that within the bulk each Wannier function is exponentially localized around its eigenvalue along \hat{x} , even for cases of nontrivial Chern number. This implies that the x_n 's of the Wannier functions that reside within the middle of the region \mathcal{A} are unaffected by details of the system out of \mathcal{A} or by the edges of \mathcal{A} .

So far we have shown that given $P(\phi = 0)$ in a local region \mathcal{A} , one has sufficient data to extract $x_n(\phi)$. In order to extract the \mathbb{Z}_2 index out of the $x_n(\phi)$'s, we follow Ref. [14] and consider the pairs of eigenvalues at $\phi = 0$ and $\phi = \pi$. As mentioned before, at these fluxes the x_n 's come in degenerate pairs. The difference between a BI and a TI is whether the pairs at $\phi = 0$ are the same as those at $\phi = \pi$ (BI) or not (TI), as depicted in Fig. 1.

The \mathbb{Z} index is even simpler to extract, since there is no degeneracy in the x_n 's, and all the 1D Wannier

functions move in the same direction [15]. According to gauge invariance, the eigenvalues at $\phi = 0$ are the same as those at $\phi = 2\pi$, but each x_n may be carried with the flux to x_m . If the labeling of the eigenvalues is such that $x_{n+1} > x_n$, then the \mathbb{Z} index equals to $m - n$, as depicted in Fig. 2.

The four \mathbb{Z}_2 indices of the 3D TI ($\nu_0; \nu_x, \nu_y, \nu_z$) can be extracted by generalizing the pair switching criterion [16]. Given a sample with periodic boundary conditions in \hat{y} and \hat{z} , the Wannier centers are carried with two independent fluxes $x_n(\phi_y, \phi_z)$, where ϕ_y (ϕ_z) corresponds to the phase twist in \hat{y} (\hat{z}). Now $\nu_y = 1$ if the pairs switch partners between $(\phi_y, \phi_z) = (\pi, 0)$ and (π, π) and, accordingly, $\nu_z = 1$ for switching between $(0, \pi)$ and (π, π) . If the pair switching in the course $(0, 0) \rightarrow (0, \pi)$ differs from that in $(\pi, 0) \rightarrow (\pi, \pi)$, then $\nu_0 = 1$. In order to extract ν_x we must have P also in a geometry that is periodic in \hat{x} and \hat{y} .

We can see that in 3D TI the geometry on which P is given plays an important role. The 3D generalization of the 2D cylinder is periodic boundary conditions in two directions, while the 3D generalization of the Corbino disk is the Corbino donut. The Corbino donut can be isolated from any given sample by discarding sites from the projector, and therefore properties inferred from these geometries must be local and isotropic. On the contrary, the 3D cylinder cannot be isolated from larger samples, and therefore properties inferred from this geometry need not be local nor isotropic. In the Corbino donut we consider only the flux that resides inside the donut, and X denotes the open radial coordinate. For $\nu_0 = 1$ we expect pair switching, since gapless states will appear at the surface [16]. On the other hand, since a Corbino donut can be isolated from a larger sample in any orientation, it is impossible to extract from it the orientation-dependent weak indices.

In the presence of interactions, the ground-state two-point correlation function remains well defined. However, it no longer corresponds to a projection matrix, which is the requested input to the process. Prior to the addition of interactions all the eigenvalues of the correlation function were either 0 or 1, corresponding to occupied and unoccupied states. One can think of this as an occupation gap of exactly 1. As interactions are gradually increased, and as long as there is no phase transition, the correlation function is expected to change continuously, and the occupation gap to remain finite. Provided that, it is possible to extract a truncated projector out of the correlation function in a way which is independent of the truncation process, as will be proven below.

In general, locality of topological order implies a bulk-edge correspondence theorem, provided that the topological order is well defined for insulating phases. Assume that two samples which belong to two different classes are attached. If the entire system remains gapped, it belongs to a single topological class. However, according to the locality of the order, the system seems to belong to two classes simultaneously. This contradiction implies

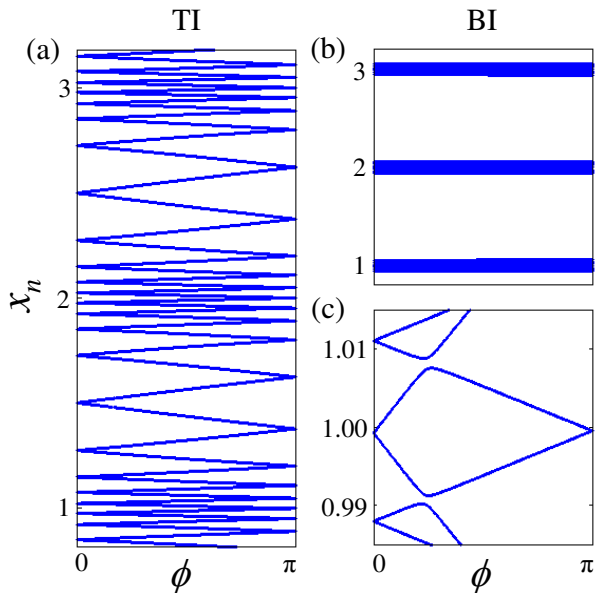


FIG. 1: The centers of the 1D Wannier functions x_n as a function of the artificial flux ϕ of the 2D Kane and Mele model, as extracted from the local two-point correlation function at $\phi = 0$, of both a topological (left) and a trivial (right) insulators. (a) In the TI the centers switch pairs between $\phi = 0$ and $\phi = \pi$. (b) In the BI the centers are essentially fixed. (c) Zooming-in shows that they actually move, but without switching pairs.

a closure of the gap, which can only take place at the interface. In the other way, if the gap can remain open between the two attached samples, the classifying order must be nonlocal. For example, weak topological insulators may have a gapped surface (in a stacking direction) [16], which means that the weak order is nonlocal, in agreement to what has been stated above.

III. NUMERICAL IMPLEMENTATIONS

The above approach can be easily adapted to a computer algorithm. For a given two-point correlation function P , one can diagonalize the matrix $PXP|_\phi$ for various fluxes, and examine the resulting eigenvalue spectrum. However, due to finite size effect, some of the eigenstates of PXP would be localized near the edges of the region \mathcal{A} . These eigenstates are edge dependent and, therefore, do not reflect the physical behavior of the bulk. Fortunately, due to the exponential localization of the eigenstates, one can easily distinguish these state from the bulk eigenstates and discard them, as proven in the Appendix.

We have carried out this process on the 2D Kane and Mele model of the TI [17] in the presence of disorder. The Hamiltonian of this model is parameterized by nearest neighbor hopping t , staggered on-site potential λ_v , S_z

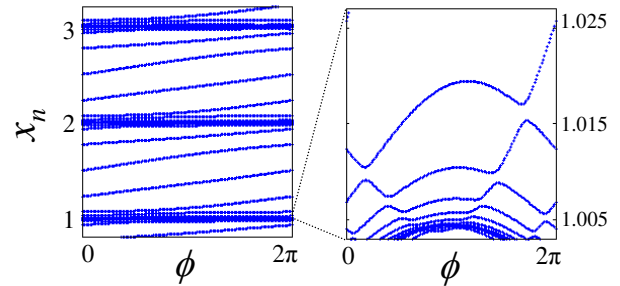


FIG. 2: The centers x_n versus the artificial flux ϕ of a single spin copy of the quantum spin Hall effect model, as extracted from P at zero flux. Each center replaces its preceding center while carried with the flux, $x_n(2\pi) = x_{n+1}(0)$, in all scales, as expected from $\nu = 1$.

conserving spin-orbit interaction λ_{SO} , and Rashba spin-orbit interaction λ_R . We took a cylindrical 18×42 lattice, with $t = 1$, $\lambda_{SO} = 0.1$, $\lambda_R = 0.05$, for the BI $\lambda_v = 0.9$, while for the TI $\lambda_v = 0.1$. Both Hamiltonians were subject to a uniformly distributed random potential of magnitude 0.1. The spectral flows $x_n(\phi)$ at the middle of the cylinder of both the trivial and topological phases are depicted in Fig. 1. The difference in the pair switching behavior is clearly visible.

Similarly, we performed the procedure on a single spin copy of the quantum spin Hall effect model [18], which is equivalent to IQHE. The parameters of this models are the hopping element of the two bands $B - D$ and $B + D$, the interband hopping A , and the energy gap M . Figure 2 depicts the movement of the 1D Wannier functions at the middle of a cylindrical 30×40 lattice, with $B = 1$, $D = 0.2$, $A = 0.4$, and $M = 0.1$, which yield $\nu = 1$. A uniform disorder of magnitude $0.3M$ is also present. It is evident that $x_n(2\pi) = x_{n+1}(0)$, which means that this insulator belongs to class 1 of the \mathbb{Z} index, as expected.

A comment is in order that different $x_n(\phi)$'s may appear to cross at accidental values between $\phi = 0$ and $\phi = \pi$; for example, see Fig. 1(c). In such cases one should relate the upper state before the crossing to the upper state after the crossing and the same for the lower. This process is equivalent to opening a gap at the crossing point by some small local perturbation. Moreover, due to Wigner noncrossing theorem [19], this gap is probably there, only it is not visible within the numerical accuracy.

IV. PROOFS OF ANALYTICAL PROPERTIES

Now we turn to prove the three properties that have been stated above. The band insulator lattice Hamiltonian H is characterized by a spectrum with a finite gap Δ around some value μ , and a maximal energy in absolute value D above μ . We also assume that H does not couple two sites which are more than l_h sites apart. Since we are interested in bulk properties, we assume that

the periodic dimensions of the lattice are of finite size L , while the open coordinate is infinite (finite size systems are discussed in the Appendix).

The starting point of the proofs is to develop a representation of the projector P as a finite polynomial in H . The projector P can also be expressed as

$$P = \lim_{\epsilon \rightarrow 0^+} \frac{1}{2} \left(1 - \operatorname{erf} \left(\frac{H - \mu}{\epsilon \Delta} \right) \right), \quad (5)$$

where $\operatorname{erf}(x)$ denotes the Taylor series of the error function. The equivalence of this expression to the definition can be easily verified in the eigenbasis of H . Accordingly, we define the approximate projector P_ϵ to be the same as P but with finite $\epsilon \ll 1$. If the error of the approximation is measured by the Euclidean norm, we can bound it by $\|P - P_\epsilon\| = (1 - \operatorname{erf}(\epsilon^{-1}))/2 < e^{-1/\epsilon^2}$.

Since the $\operatorname{erf}(x)$ is an entire function, P_ϵ can be approximated by taking only the N first terms of the series

$$P_{N,\epsilon} = \frac{1}{2} \left(1 - \frac{2}{\sqrt{\pi}} \sum_{n=0}^N \frac{(-1)^n}{n!(2n+1)} \left(\frac{H - \mu}{\epsilon \Delta} \right)^{2n+1} \right). \quad (6)$$

According to Taylor's theorem there exists $x_0 \in (0, (D/\Delta)\epsilon^{-1})$ such that $\|P_\epsilon - P_{N,\epsilon}\| = x_0^{2N+3}/[\sqrt{\pi}(N+1)!(2N+3)]$. By using Stirling's approximation, and choosing $N_\epsilon = e^2(D/\Delta)^2\epsilon^{-2} \gg \epsilon^{-2}$, we can bound

$$\|P_\epsilon - P_{N,\epsilon}\| < \frac{D}{\sqrt{N}\Delta\epsilon} \left(\frac{eD^2}{N\Delta^2\epsilon^2} \right)^{N+1} = e^{-N_\epsilon}. \quad (7)$$

Consequently, we can conclude that $P_{N_\epsilon,\epsilon}$ is an excellent approximation of P , with an error of $\|P - P_{N_\epsilon,\epsilon}\| < e^{-1/\epsilon^2} \equiv e^{-Q}$, with Q as the measure of the accuracy. Therefore, in order to approximate P with accuracy Q , it is sufficient to take $N_Q = e^2(D/\Delta)^2Q$ terms.

Property I: P_{ij} decays exponentially with the distance between i and j within some correlation length l_p , and has only an exponentially small dependence on the Hamiltonian outside a local region around i and j .

Proof: According to the assumptions, $[H^{2N+1}]_{ij}$ vanishes for two sites i, j which are separated a distance $r_{ij} > (2N+1)l_h \approx 2Nl_h$. Accordingly, $[P_{N,\epsilon}]_{ij}$ also vanishes, while P_{ij} may be of order $e^{-Q(N)}$. Therefore, for a given $r_{ij} > 2l_h$, we choose $N = \lceil r_{ij}/2l_h \rceil$, which keeps $[P_{N,\epsilon}]_{ij}$ as zero, while giving a maximal $Q(N)$. Following this choice one finds that

$$|P_{ij}| < e^{-r_{ij}/l_p}, \quad (8)$$

$$l_p = 2e^2(D/\Delta)^2l_h. \quad (9)$$

Moreover, P_{ij} for two sites within a certain region \mathcal{A} does not depend on the matrix elements H_{kl} of two sites within region \mathcal{B} as long as the distance between \mathcal{A} and \mathcal{B} is much larger than l_p . This can be shown by choosing $N = r_{\mathcal{A}\mathcal{B}}/2l_h$, where $r_{\mathcal{A}\mathcal{B}}$ is the minimal distance between

\mathcal{A} and \mathcal{B} . Now $[P_{N,\epsilon}]_{ij}$ does not depend on H_{kl} , and P_{ij} may depend on it on the order of $e^{-r_{\mathcal{A}\mathcal{B}}/l_p}$ [20].

This way of creating an exponentially local projector from the Hamiltonian can be performed on any gapped matrix with a finite band width. In particular the two-point correlation function of a weakly interacting system can be deformed into a projector, as required for the index determining procedure, as long as the occupation gap remains finite.

Property II: Magnetic flux which threads a cylinder or a torus affects P_{ij} by a simple geometric phase factor.

Proof: Insertion of the magnetic flux Φ affects H in the uniform gauge by

$$H_{kl}(\Phi) = H_{kl} e^{i2\pi y_{kl}\Phi/L\Phi_0}, \quad (10)$$

where $y_{kl} \in (-L/2, L/2]$ is the azimuthal distance from site k to site l , and Φ_0 is the flux quanta. Consider H_{kl} within a region \mathcal{C} that cover less than a half of the circumference of the cylinder or the torus. One can adopt a convention for the coordinate $y \in (0, L)$ that avoids the branch cut inside \mathcal{C} and write $y_{kl} = y_k - y_l$. Within \mathcal{C} Eq. (10) can now be written as a unitary transformation

$$H(\Phi)|_{\mathcal{C}} = U(\Phi) H U^\dagger(\Phi)|_{\mathcal{C}}, \quad (11)$$

$$U_{kl}(\Phi) = \delta_{kl} e^{i2\pi y_k \Phi/L\Phi_0}, \quad k, l \in \mathcal{C}. \quad (12)$$

Given P_{ij} , we can approximate it by $N = L/4l_h$ terms. Since $[P_{N,\epsilon}]_{ij}$ does not vanish only for $r_{ij} \sim l_p \ll L$, it depends on H_{jk} only for j, k within a region of size $L/2$, which covers not more than a half of the circumference. Hence we may substitute Eq. (11) in Eq. (6) and obtain Eq. (3) by identifying $\phi = \Phi/\Phi_0$ and $\theta_{ij} = 2\pi y_{ij}/L$.

Property III: The 1D Wannier functions, defined as eigenstates of the operator PXP , are exponentially localized in the \hat{x} direction around the corresponding eigenvalues.

Proof: Consider the action of the projector P on some normalized state $|a\rangle$ which is localized around x_a within a width l_a . Since P_{ij} is local with width l_p , $P|a\rangle$ is still localized at the vicinity of x_a , but it might be as wide as $l_a + l_p$. Note that $P|a\rangle$ is not necessarily normalized to 1 but may have a smaller norm. Since the position operator X is diagonal in the position basis, $(X - x_a)|a\rangle$ is localized almost in the same manner as $|a\rangle$, but its norm may increase up to $2l_a$.

Following this, if we begin with a particle at site i , and apply $P(X - x_i)P$ on it, then $\|P(X - x_i)P|i\rangle\| < 2l_p$. Applying it M times yields $\|(P(X - x_i)P)^M|i\rangle\| < (2l_p)^M M! \approx \sqrt{2\pi M} (2l_p M/e)^M$.

Now let $|w_n\rangle$ be an eigenstate of PXP with eigenvalue $x_n \neq 0$, and consider $|i\rangle$ with $|x_n - x_i| > 2l_p$. It can be shown that $P|w_n\rangle = |w_n\rangle$, yielding $\langle i|w_n\rangle = (x_n - x_i)^{-M} \langle i|(P(X - x_i)P)^M|w_n\rangle$. Following the inequality $|\langle a|b\rangle| \leq \|a\| \cdot \|b\|$, we have $|\langle i|w_n\rangle| < \sqrt{2\pi M} [2l_p M/(e(x_n - x_i))]^M$. For given x_n and x_i we choose $M = \lceil |x_i - x_n|/2l_p \rceil$, and get the exponential lo-

calization of the 1D Wannier function [21]

$$|\langle i|w_n\rangle| < \sqrt{\pi|x_i - x_n|/l_p} e^{-|x_i - x_n|/2l_p}. \quad (13)$$

V. CONCLUSION

To conclude, in this work we proved that the \mathbb{Z} and \mathbb{Z}_2 topological indices can be extracted from the ground-state equal-time two-point correlation function at zero flux, given on any section larger than some correlation length. This implies that the order in such topological phases can be thought of as a local ground-state property. In the case of 3D TI it was suggested that the strong index is indeed local in the above sense, while the weak indices carries some global information.

Heuristically, one can reach a similar conclusion using entanglement spectrum [22]. Indeed, P_{ij} on a finite region is related to the reduced density matrix. A gapless spectrum of P_{ij} is therefore an indication of nontrivial topology [23, 24]. Nevertheless, given a finite region one cannot differentiate a gapped spectrum from a gapless one without inserting fluxes.

It will be interesting to establish this approach in interacting systems and to apply it on fractional quantum Hall states. Preliminary numerical results indicate that the electron two-point correlation function of the ground state at filling factor 1/3 is proportional to the one of filling factor 1. Hence, it may be possible to extract the topological order of fractional states in a similar way.

We hope that our viewpoint will encourage the efforts for finding manifestations of the \mathbb{Z}_2 index through local bulk properties.

ACKNOWLEDGEMENTS

We thank Ady Stern and Ehud Altman for useful discussions. Z.R. thanks A. Soroker, and Y.E.K. thanks M. Kraus. Z.R. Acknowledges ISF Grant No. 700822030182, and Y.E.K. thanks the U.S.-Israel Binational Science Foundation and the Minerva foundation for financial support.

Appendix A: Edge effects

In the main text we avoided edge effects by considering geometries with periodic dimensions and an infinite open coordinate. In practice, a finite open coordinate must be used, causing numerical artifacts that should be filtered out in order to reveal the bulk behavior. This can be done in a controlled manner provided that the 1D Wannier functions of the bulk and the edge are distinguishable. The first part of this Appendix establishes this distinction, and the second part presents the actual numerical procedure.

The starting point of the proofs in Sec. IV was expanding the spectral projector P as a series in powers of the Hamiltonian H , with the spectral gap Δ as a control parameter. An edge may give rise to gapless edge states and so our first task is to establish the expansion in the presence of such states.

We assume that H is characterized as before, only now the spectrum of H includes both bulk states with energy greater than the gap, and edge states with subgap energy, which are exponentially localized along the edge. The projector P can then be divided into bulk and edge parts

$$\begin{aligned} P &= P^{bulk} + P^{edge} \\ &= \sum_{E_n < \mu - \Delta} |n\rangle\langle n| + \sum_{\mu - \Delta < E_n < \mu} |n\rangle\langle n|, \end{aligned} \quad (A1)$$

where $|n\rangle$ denotes an eigenstate with eigenvalue E_n , and μ is the chemical potential, as before. Since P^{edge} is composed only of the edge states, it decays exponentially into the bulk. Therefore $[P^{edge}]_{ij}$ is exponentially small, if either i or j (or both) reside within the bulk.

In a similar manner to what we have done above, we introduce an error function approximation to the projector

$$\begin{aligned} P_\epsilon &= P_\epsilon^{bulk} + P_\epsilon^{edge} \\ &= \sum_{E_n < \mu - \Delta} \frac{1}{2} \left(1 - \operatorname{erf} \left(\frac{E_n - \mu}{\epsilon \Delta} \right) \right) |n\rangle\langle n| \\ &+ \sum_{\mu - \Delta < E_n < \mu} \frac{1}{2} \left(1 + \operatorname{erf} \left(\frac{E_n - \mu}{\epsilon \Delta} \right) \right) |n\rangle\langle n|. \end{aligned} \quad (A2)$$

We can see that $\|P^{bulk} - P_\epsilon^{bulk}\| < e^{-1/\epsilon^2}$ as before, while P_ϵ^{edge} is a poor approximation to P^{edge} , since the summation coefficients spread from 0 to 1. Indeed P_ϵ^{edge} is a poor approximation of P^{edge} at the edge. However, within the bulk both $[P_\epsilon^{edge}]_{ij}$ and $[P^{edge}]_{ij}$ are exponentially small, and therefore also the error $|[P_\epsilon^{edge} - P^{edge}]_{ij}|$.

This implies that for bulk-bulk or bulk-edge correlation, P may still be approximated by P_ϵ within an exponential accuracy. P_ϵ can be Taylor expanded up to some finite order N , and by choosing optimal values for ϵ and N we can bound the error. Since this part of the proof is unaffected by the edges, we refer the reader back to Sec. IV. We turn to discuss the effect of edges on properties I–III.

Property I (the exponential locality of P) relies on the serial expansion, and therefore is valid only within the bulk. Nevertheless, since the edge states decay into the bulk, P decays exponentially also at the vicinity of the edge but only perpendicularly to the edge.

Property II (the artificial flux insertion) is valid as long as P decays along the periodic coordinates, which does not necessarily happen in the presence of edge states. Thus the artificial flux insertion approximation is valid only far from the edge.

Property III states that the 1D Wannier functions are exponentially localized around their eigenvalues along the open coordinate X . As long as the 1D Wannier functions are produced by diagonalizing PXP , and P is a true projection operator over the entire physical system, the proof remains unchanged in the presence of edges. Nevertheless, we do not wish to limit ourselves to cases in which the entire P matrix is known, since this is not a local quantity. Our algorithm uses P which is given on some local area with a geometry of a cylinder or a Corbino disk. But P which is truncated to some local region is generally not a projection matrix.

The projection property $P^2 = P$ was used in the original proof only once, when it was stated that it can be shown that $P|w_n\rangle = |w_n\rangle$, where $|w_n\rangle$ is an eigenfunction of PXP with eigenvalue $x_n \neq 0$. This property was required in order to establish the equality

$$\langle i|w_n\rangle = (x_n - x_i)^{-M} \langle i|(P(X - x_i)P)^M|w_n\rangle, \quad (\text{A4})$$

where $|i\rangle$ is a state localized at site i . If the truncated P is no longer a projector, then $[PXP, P] \neq 0$, and $|w_n\rangle$ may not be an eigenstate of P . But since we are interested in bulk properties, it suffices to prove that Eq. (A4) is valid far from the edges of P (which may differ from the physical edges due to the truncation).

It is useful to divide the system into three groups: \mathcal{S} will denote the entire system, $\mathcal{A} \subset \mathcal{S}$ the truncation area, and $\mathcal{B} \subset \mathcal{A}$ the inner region of \mathcal{A} , which will be defined by the set of all sites which are far from the edges of \mathcal{A} , on the scale of the correlation length l_p . Recall that P is a piece of the true projector of the entire system, which we denote by \tilde{P} . Following the locality of P , we find that for i or j in \mathcal{B}

$$\begin{aligned} [P^2]_{ij} &= \sum_{k \in \mathcal{A}} P_{ik} P_{kj} = \sum_{k \in \mathcal{A}} \tilde{P}_{ik} \tilde{P}_{kj} \\ &\approx \sum_{k \in \mathcal{S}} \tilde{P}_{ik} \tilde{P}_{kj} = \tilde{P}_{ij} = P_{ij}, \end{aligned} \quad (\text{A5})$$

up to corrections that are exponentially small in the distance between the site in \mathcal{B} and the edge of \mathcal{A} , divided by l_p . We can see that P is still a projector up to boundary effects.

Since P is approximately a projector within \mathcal{B} ,

$$\begin{aligned} \langle i|P|w_n\rangle &= (1/x_n) \langle i|PPXP|w_n\rangle \\ &\approx (1/x_n) \langle i|PXP|w_n\rangle = \langle i|w_n\rangle \quad \forall i \in \mathcal{B}, \end{aligned} \quad (\text{A6})$$

for $x_n \neq 0$. This means that as far as region \mathcal{B} is considered, $|w_n\rangle$ is indeed an eigenstate of P . Seemingly we recovered Eq. (A4) for any site i within \mathcal{B} . However, $(P(X - x_i)P)^M|i\rangle$ may be as wide as $M \cdot 2l_p$, which restricts the validity of Eq. (A4) to $M < d(i, \mathcal{B})/2l_p$, where $d(i, \mathcal{B})$ is the distance between site i and the edge of \mathcal{B} .

The exponential localization of $|w_n\rangle$ around x_n was achieved by choosing $M = \lceil |x_i - x_n|/2l_p \rceil$. The restriction on M is then translated to a restriction on the exponential localization to be valid only for $|x_i - x_n| < d(i, \mathcal{B})$, although x_i and x_n are both in \mathcal{B} .

So far we have shown that for x_n in \mathcal{B} , its eigenfunction $|w_n\rangle$ decays exponentially with the distance. Note that this does not exclude the possibilities that $|w_n\rangle$ resides at the edge of \mathcal{A} , or both at the edge and around x_n . The last scenario is, however, highly nongeneric. Assume that some $|w_n\rangle$ is indeed doubly localized in that fashion. Up to exponential accuracy we may split it into sum of two functions $|w_n\rangle = |w_n, \mathcal{B}\rangle + |w_n, \mathcal{A}\rangle$, where $|w_n, \mathcal{B}\rangle$ is localized around x_n and $|w_n, \mathcal{A}\rangle$ is localized around the edge. Since PXP is local, it does not couple these two functions, and $|\tilde{w}_n\rangle = |w_n, \mathcal{B}\rangle - |w_n, \mathcal{A}\rangle$ is also an eigenfunction, with an eigenvalue that is exponentially close to x_n . Such an almost degeneracy is of course nongeneric.

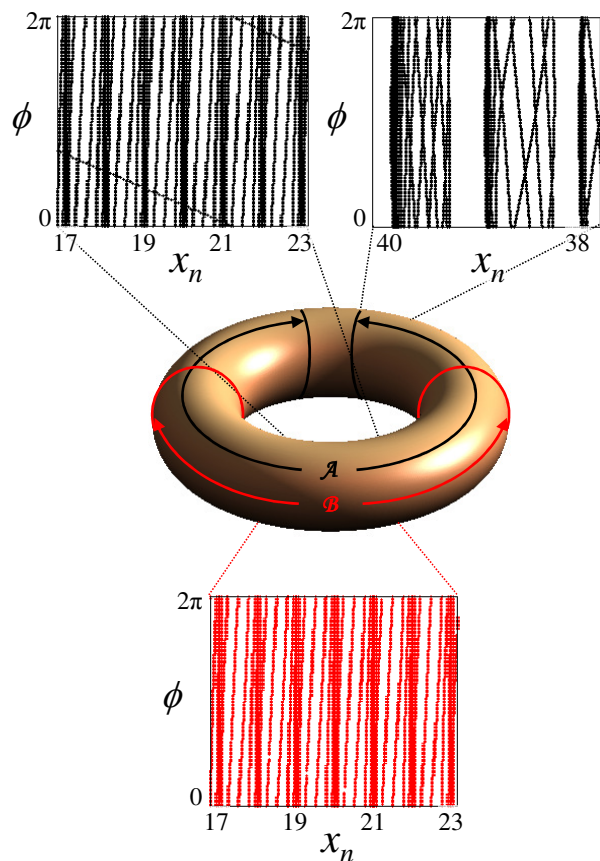


FIG. 3: Demonstration of bulk-edge separation in the single spin copy of the quantum spin Hall effect. The projector P was created by truncating a 30×34 cylinder, denoted by \mathcal{A} , from the 30×40 torus. The full spectrum of $PXP|_\phi$ (top, black) is trivial both in the bulk and at the edge. Omitting states that are localized at the edges gives a pure bulk spectrum at region \mathcal{B} (bottom, red), which is indeed nontrivial.

To conclude, we have seen that edges do not affect the bulk properties of P . Moreover, the 1D Wannier function with eigenvalue in the bulk are localized either around their eigenvalue or at the edge. Therefore, given the correlation function P on an arbitrary geometry, one can isolate/truncate a cylinder or a Corbino disk from

it and distinguish the 1D Wannier functions that reside within the bulk. Due to their localization properties, the 1D Wannier functions are unaffected by the edges or the truncation process, and the motion of their eigenvalues as a function of the flux is therefore purely a bulk property.

We now demonstrate how these analytical statements are exploited in the computer algorithm. For that purpose we fully diagonalized the Hamiltonian of the single spin copy of the quantum spin Hall effect, for a periodic 30×40 lattice, with the parameters that are given in Sec. III. The projector P was then produced by summing all projectors on the states with negative energy and was characterized by a correlation length of approximately 2. Region \mathcal{A} was chosen to be a 30×34 cylinder out of the full torus, and all the elements P_{ij} with i and j out of \mathcal{A} were omitted.

The next step was to construct the spectrum $\{x_n(\phi)\}$

by diagonalizing $PXP|_\phi$, where X in region \mathcal{A} ranged from 4 to 37. The full spectrum is trivial, as depicted at the top of Fig. 3. At the edges of \mathcal{A} edge states hybridize with the outmost bulk states, and gaps are opened. At the center of \mathcal{A} most eigenvalues belong to bulk states, while the branch of eigenvalues that crosses the spectrum from side to side belongs to an edge state.

In order to remain with bulk effects only, we used the localization property of the 1D Wannier functions, which guarantees that the bulk wave functions are localized within the middle of region \mathcal{A} , denoted above by \mathcal{B} . We chose \mathcal{B} to be the central cylinder of 20 sites, and discarded all the 1D Wannier functions that more than 5% of their weight is outside \mathcal{B} . In this way we assured that all the states in \mathcal{B} are purely bulk states, and the nontrivial nature of the spectrum became apparent, as seen in the bottom of Fig. 3.

-
- [1] M.Z. Hasan and C.L. Kane, *Rev. Mod. Phys.* **82**, 3045 (2010).
 - [2] E.M. Lifshitz and L.P. Pitaevskii, *Statistical Physics*, (Pergamon, Oxford, UK, 1980), Pt. 1,
 - [3] Since the IQHE is widely accepted as a topologically ordered phase, and since TI are close relatives of IQHE, we allow ourselves to call them “topologically ordered”; see also S. Ryu, A.P. Schnyder, A. Furusaki and A.W.W. Ludwig, *New J. Phys.* **12**, 065010 (2010).
 - [4] Q. Niu and D.J. Thouless, *Phys. Rev. B* **35**, 2188 (1987).
 - [5] X.L. Qi, R. Li, J. Zang and S.C. Zhang, *Science* **323**, 1184 (2009).
 - [6] W.K. Tse and A.H. MacDonald, *Phys. Rev. Lett.* **105**, 057401 (2010).
 - [7] D. Hsieh, D. Qian, L. Wray, Y. Xia, Y.S. Hor, R.J. Cava and M.Z. Hasan, *Nature* **452**, 970 (2008).
 - [8] Y. Ran, Y. Zhang and A. Vishwanath, *Nat. Phys.* **5**, 298 (2009).
 - [9] Q. Niu, D.J. Thouless and Y.S. Wu, *Phys. Rev. B* **31**, 3372 (1985).
 - [10] L. Fidkowski and A. Kitaev, *Phys. Rev. B* **81**, 134509 (2010).
 - [11] G.E. Volovik, *JETP Lett.* **90**, 587 (2009).
 - [12] Consequently, using the above equation for two fluxes in the expression for the Chern number, $\nu = \frac{1}{2\pi i} \int d\phi_x d\phi_y \text{Tr}(P, [\partial_{\phi_x} P, \partial_{\phi_y} P])$, reveals that the integration over the flux is superfluous.
 - [13] S. Kivelson, *Phys. Rev. B* **26**, 4269 (1982).
 - [14] L. Fu and C.L. Kane, *Phys. Rev. B* **74**, 195312 (2006).
 - [15] J. Zak, *Phys. Rev. Lett.* **62**, 2747 (1989).
 - [16] L. Fu, C.L. Kane and E.J. Mele, *Phys. Rev. Lett.* **98**, 106803 (2007).
 - [17] C.L. Kane and E.J. Mele, *Phys. Rev. Lett.* **95**, 146802 (2005).
 - [18] B.A. Bernevig, T.L. Hughes and S.C. Zhang, *Science* **314**, 1757 (2006).
 - [19] J. von Neumann and E.P. Wigner, *Phys. Z* **30**, 467, (1927).
 - [20] These results are related to previous works of Hastings, for example M.B. Hastings, *Phys. Rev. B* **73**, 085115 (2006). However, the local dependence of P on H , and the natural generalization to any gapped matrix are new. Furthermore, our way of getting these results is more direct.
 - [21] H.D. Cornean, A. Nenciu and G. Nenciu, *J. Phys. A: Math. Theor.* **41**, 125202 (2008) reached a similar conclusion for continuum models.
 - [22] H. Li and F.D.M. Haldane, *Phys. Rev. Lett.* **101**, 010504 (2008).
 - [23] A.M. Turner, Y. Zhang and A. Vishwanath, *Phys. Rev. B* **82**, 241102(R) (2010).
 - [24] E. Prodan, T.L. Hughes and B.A. Bernevig, *Phys. Rev. Lett.* **105**, 115501 (2010).